Supporting Information

Imidazo[2,1-*b*]benzothiazol derivatives as potential allosteric inhibitors of the glucocorticoid receptor

Michael S Christodoulou, Federico Dapiaggi, Francesca Ghiringhelli, Stefano Pieraccini, Maurizio Sironi, Marianna Lucafò, Debora Curci, Giuliana Decorti, Gabriele Stocco, Chandra Sekhar Chirumamilla, Wim Vanden Berghe, Patrick Balaguer, Benoit Y. Michel, Alain Burger, Egle M. Beccalli, Daniele Passarella and Nadine Martinet

General procedures

All reactions were carried out in oven-dried glassware and dry solvents under nitrogen atmosphere. All solvents were purchased from Sigma Aldrich and used without further purification. Substrates and reagents were purchased from Sigma Aldrich and used as received. Thin layer chromatography (TLC) was performed on Merck precoated $60F_{254}$ plates. Reactions were monitored by TLC on silica gel, with detection by UV light (254 nm). Flash chromatography was performed using silica gel (240-400 mesh, Merck). All tested compounds had a purity of > 98% confirmed via elemental analyses (CHN) in a Perkin Elmer 2400 instrument. ^{1}H-NMR spectra were recorded on a Bruker DRX-400 instrument and are reported relative to residual $CDCl_3$ and DMSO. ^{13}C-NMR spectra were recorded on the same instrument (100 MHz) and are reported relative to residual $CDCl_3$ and DMSO. Chemical shifts (δ) for proton and carbon resonances are quoted in parts per million (ppm) relative to tetramethylsilane (TMS), which was used as an internal standard. MS spectra were recorded using the electrospray ionization (ESI) technique on a Waters Micromass Q-Tof micro mass spectrometer.

Compounds **1**-**10** were synthesized in a previous work.[1] Compound **11** was easily prepared by hydrolysis of compound **9** in the presence of NaOH with an excellent yield (95%). Esterification of compound **11** using trimethylsilyldiazomethane provided compound **12** with a good yield (60%) (Scheme 1). Compound **13** was obtained by condensation of the easily prepared 2-amino-5,6-dihydrobenzo[*d*]thiazol-7(4*H*)-one[2] with 2-Br-4'-CN-acetophenone with a low yield (20%) (Scheme 2).

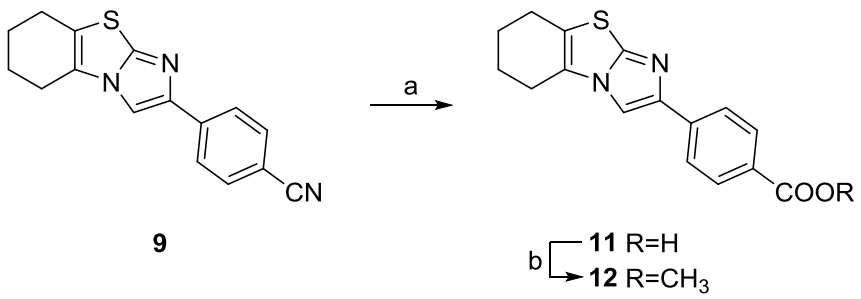

Scheme 1. a) NaOH, EtOH, H_2O, reflux 5 h; b) trimethylsilyldiazomethane, MeOH, 2 h, r.t.

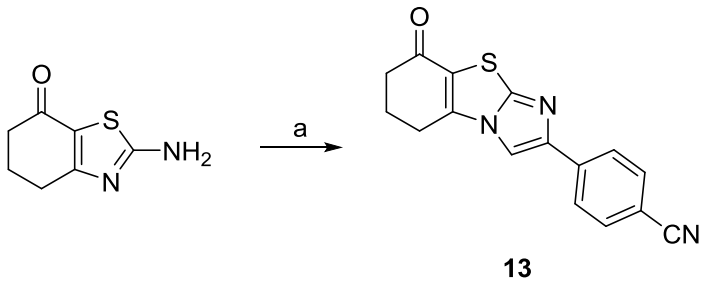

Scheme 2. a) 2-Br-4'-CN-acetophenone, EtOH, reflux 3 h.

Synthesis of 4-(5,6,7,8-tetrahydroimidazo[2,1-*b*]benzothiazol-2-yl)benzoic acid (11). To a solution of 4-(5,6,7,8-tetrahydroimidazo[2,1-*b*]benzothiazol-2-yl)benzonitrile (**9**) (0.20 g, 0.72 mmol) in EtOH/H_2O (4/4 mL), NaOH (0.37 g, 9.1 mmol) was added and the solution was refluxed for 5 h. Then, the solvents were evaporated and 35 mL of H_2O and 5 mL of HCl 3M were added. The formed precipitate was filtered, washed with DEE and dried overnight under P_2O_5 atmosphere, to provide compound **11** as white amorphous solid (95% yield). R_f = 0.19 (EtOAc); ^{1}H NMR (DMSO-d_6): δ = 8.29 (1H, s), 7.91 – 7.89 (4H, m), 2.72 – 2.66 (4H, m), 1.92 – 1.86 (4H, m); ^{13}C NMR (DMSO-d_6): δ = 168.1, 147.4, 144.8, 137.6, 132.8, 128.4 (2C), 126.8, 124.5 (2C), 121.5, 109.1, 24.27, 23.13, 22.60, 21.61; MS: 299.37 ($M+H^+$); Anal. Calcd for $C_{16}H_{14}N_2O_2S$: C, 64.41; H, 4.73; N, 9.39. Found: C, 64.17; H, 4.65; N, 8.94.

Synthesis of methyl 4-(5,6,7,8-tetrahydroimidazo[2,1-*b*]benzothiazol-2-yl)benzoate (12). To a solution of compound **11** (0.16 g, 0.55 mmol) in MeOH (5.3 mL), a solution of trimethylsilyldiazomethane (1.3 mL, 2M in Hexane) was added and the solution was stirred at r.t. for 2 h. After the completion of the reaction, the solvent was evaporated, EtOAc was added and the organic phase was washed with brine, dried with Na2SO4, filtered and evaporated. The residue was purified by flash column chromatography (EtOAc) to provide compound **12** as white amorphous solid (60% yield). R_f = 0.60 (EtOAc); ^{1}H NMR ($CDCl_3$): δ = 8.07 (2H, d, J = 8.8 Hz), 7.91 (2H, d, J = 8.8 Hz), 7.65 (1H, s), 3.94 (3H, s), 2.74 – 2.67 (4H, m), 2.01 – 1.94 (4H, m); ^{13}C NMR ($CDCl_3$): δ = 167.7, 145.8, 139.4, 133.1, 130.7 (2C), 128.7, 126.4, 125.3 (2C), 123.2, 107.5, 52.65, 24.99, 23.74, 23.28, 22.31; MS: 313.40 ($M+H^+$); Anal. Calcd for $C_{17}H_{16}N_2O_2S$: C, 65.36; H, 5.16; N, 8.97. Found: C, 64.72; H, 5.09; N, 8.95.

Synthesis of 4-(8-oxo-5,6,7,8-tetrahydroimidazo[2,1-*b*]benzothiazol-2-yl)benzonitrile (13). To a solution of 2-amino-5,6-dihydrobenzo[*d*]thiazol-7(4*H*)-one (0.74 g, 4.4 mmol) in EtOH (69 mL), 2-Br-4'-CN-acetophenone (1.48 g, 6.6 mmol) was added and the solution was refluxed for 3 h. After the completion of the reaction, the solution was cooled to 0 °C. The resulting precipitate was filtered and washed with EtOH to provide compound **13** as white amorphous solid (20% yield). R_f = 0.29 (EtOAc); ^{1}H NMR (DMSO-d_6): δ = 8.71 (1H, s), 8.05 (2H, d, J = 8.0 Hz), 7.89 (2H, d, J = 8.0 Hz), 3.13 – 3.07 (2H, m), 2.67 – 2.61 (2H, m), 2.30 – 2.23 (2H, m); ^{13}C NMR (DMSO-d_6): δ = 192.1, 149.7, 146.4, 145.6, 138.3, 133.3 (2C), 125.9 (2C), 122.8, 119.2, 111.9, 110.2, 37.42, 23.18, 21.94; MS: 294.35 ($M+H^+$); Anal. Calcd for $C_{16}H_{11}N_3OS$: C, 65.51; H, 3.78; N, 14.32. Found: C, 64.86; H, 3.72; N, 14.28.

In silico studies

GCR ligand binding domain X-ray structure was obtained from the Protein Data Bank (PDB ID 1M2Z).[3] The pocket analysis and the docking calculations were performed only on one of the two monomers in the asymmetric unit, labelled chain A. DEX was removed from the structure before docking our compounds. For the pocket analysis the EPOS software was used. Docking was carried out with Autodock 4.2,[4] employing a Lamarkian genetic algorithm.[5] 100 independent runs per molecule were performed. In each run, a population of 50 individuals evolved along 27000 generations and a maximum number of 25 million energy evaluations were performed. The best fit (lowest docked energy) solutions of the 100 independent runs were stored for subsequent analysis. The visual inspection of docked structures was carried out using VMD.[6]

GCR and NF-kB Reporter gene studies

In order to compare GCR transactivation (agonism versus antagonism) and transrepression (anti-inflammatory) properties of the different compounds, we performed GRE- and NF-κB-luciferase dependent reporter gene studies in stable transfected TNF-sensitive fibrosarcoma cells, as previously described.[7] Briefly, cells expressing $p(GRE)_2$50-Luc or $p(NF\text{-}\kappa B)_3$50-Luc were cultured in DMEM medium with 1% L-glutamine, supplemented with 10% feral bovine serum (FBS), 100 µg/mL streptomycin and 100 IU/mL penicillin in a humidified 5% CO_2 atmosphere. Cells were passaged every two days at a dilution of 1:6. Reporter gene cells were plated at a density of 0.5 x 10^5 cells/well in 24 well plates and grown overnight. $p(GRE)_2$50-Luc dependent reporter gene cells were treated with DMSO solvent, 1 µM Dex, 0.1 µM of the single compounds (GCR agonist screening), or combination treatment of Dex + single compounds (GCR antagonist screening) for 6 h. In case of $p(NF\text{-}\kappa B)_3$50-Luc, TNF (2500 IU/mL) was added for 4 h, 2 h following single compound (1 µM) treatment. After 6 h induction, media was removed from treated cells and cells were washed twice with PBS followed by addition of 100 µL of 1x lysis buffer (0.2M K_2HPO_4, 0.2M KH_2PO_4, Triton X-100, pH 7.6). Corresponding lysates of all setups were assayed for luciferase activity by adding 50 µL of luciferase assay reagents (1 mM D-luciferin salt, 3 mM ATP and 15 mM $MgSO_4$ in 30 mM HEPES buffer, pH 7.8) with 10 s mixing and measuring bioluminescence using an Envision multilabel reader(Perkin Elmer).

The stably transfected luciferase reporter HMLN cell line was obtained by stable transfection of HeLa cells with the glucocorticoid responsive gene,[8] MMTV-Luc-SV-Neo. HMLN cells were seeded at a density of 50,000 cells per well in 96-well white opaque tissue culture plates in DMEM-F12 culture medium. Test compounds were added 8 h after seeding. Cell lines were incubated for 16 h with the compounds. At the end of incubation, the medium containing test compounds was removed and replaced by culture medium containing 0.3 mM luciferin. At this concentration, luciferin diffused into the cell and produced a stable luminescent signal 5 min later. The 96-well plate was then introduced into a Microbeta Wallac luminometer and luminescence was measured in intact living cells for 2 s.

Cell viability analysis

The HeLa human cervical carcinoma (ATCC, CCL-2) cell line was grown in RPMI 1640 medium (Sigma-Aldrich, St. Louis, MO, USA) supplemented with 10% fetal calf serum, 1% L-glutamine (200 mM), 1% penicillin (10000 UI/mL) and streptomycin 10 mg/mL. Cell culture was maintained according to standard procedures in a humidified incubator at 37 °C and with 5% CO_2, and cell passage was performed once a week. For cell viability assay, HeLa cells were harvested by trypsinization and seeded into 96-well culture plates at approximately $5x10^3$ cells per well. After 24 h incubation, different concentrations of **9**, **10**, **11**, **12** and **13** compounds (250, 50, 10, 2 and 0.4 µM) dissolved in culture medium were added to each well. Then the samples were incubated for 72 h at 37 °C in the humidified atmosphere (5 % CO_2). The colorimetric 3-(4,5-dimethylthiazol-2-yl)-2,5-diphenyl tetrazolium bromide (MTT) assay was performed to assess the metabolic activity of treated cells. 20 µl stock MTT (5 mg/mL) were added to each well, and cells were then incubated for 4 h at 37 °C. Cells were lysed with isopropanol HCl 0.04 N. Absorbance was measured at 540 and 630 nm using an automated microplate reader EL311, BIOTEK ® Instruments, Vermont, USA. All measurements were done in triplicate and at least three independent experiments were carried out.

RNA isolation and quantitative real-time PCR (TaqMan®)

Total RNA was extracted using TRIzol reagent (Thermo Scientific, Carlsbad, CA, USA) according to the manufacturer's instructions. The RNA concentration and purity were evaluated by the Nano Drop instrument (NanoDrop 2000, EuroClone®, Milan, Italy). Expression levels of NR3C1 (GCRα) and GILZ genes were measured by real-time RT-PCR TaqMan® analysis using the CFX96 real-time system-C1000 Thermal Cycler (Bio-Rad Laboratories, USA). The reverse transcription reaction was carried out with the High Capacity RNA-to-cDNA Kit (Applied Biosystem, Carlsbad, CA, USA) and the real-time PCR was performed in triplicate using the TaqMan® Gene Expression Assay to assess NR3C1 and GILZ mRNAs expression, according to the manufacturer's instructions. The expression levels of the selected transcripts were determined using the comparative 2-ΔΔCt method and normalized using 18S RNA as the reference gene. The results are provided as the mean and standard deviation of three replicates experiments.

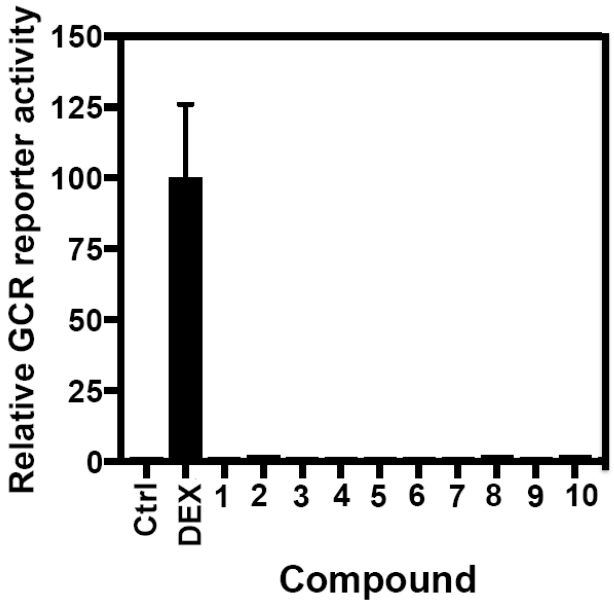

Supplementary Figure S1. GCR agonistic effects of tested compounds.

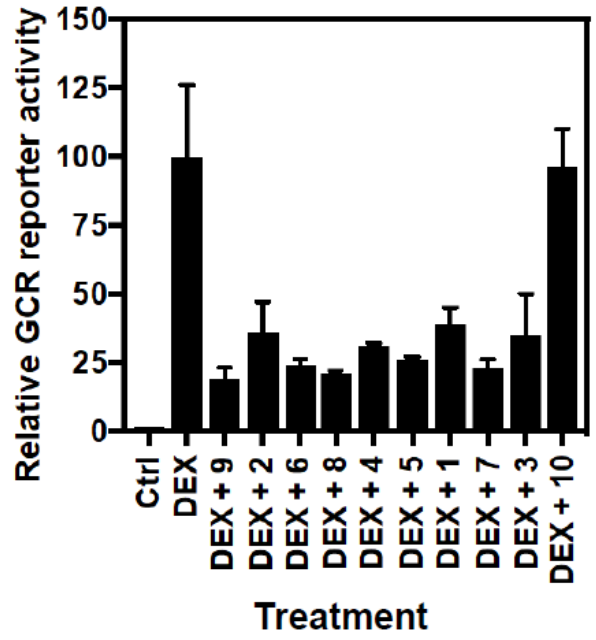

Supplementary Figure S2. GRE luc reporter gene assay of tested compounds in combination with DEX.

Supplementary Table S1. GCR crystallographic pockets, detected with EPOS. Pocket 0 corresponds to DEX binding site.

Pocked ID	Volume / Å^3	Polarity	Depth / Å
0 (DEX binding site)	660.055	0.286	2.088
1	513.031	0.340	6.576
2	419.795	0.344	15.464
3	488.004	0.330	5.136
4	641.983	0.301	5.802
5	503.956	0.327	2.353
6	517.834	0.354	6.029
7	726.703	0.312	4.782
8	320.614	0.444	5.728
9	464.319	0.361	7.044
10	415.892	0.353	5.636
11	291.588	0.381	5.514
12	267.175	0.283	7.189
13	210.373	0.275	3.866

Supplementary Table S2. Docking results. In the vast majority of the cases we obtained a unique cluster or a very high populated one, which testifies the reliability of the poses.

Pocket ID	Molecule ID	Cluster	E / kcal mol^{-1}
	9	100	-7.31
	11	100	-7.98
0	**12**	100	-7.58
	13	100	-7.67
	9	100	-5.07
	11	100	-4.95
1	**12**	98	-5.80

	13	100	-5.42
	9	100	-4.50
	11	100	-6.57
2	**12**	100	-5.58
	13	100	-5.31
	9	100	-4.95
	11	100	-6.49
3	**12**	87	-5.58
	13	95	-5.50
	9	100	-4.29
	11	100	-6.28
4	**12**	99	-5.11
	13	100	-4.69
	9	100	-2.47
	11	100	-5.19
5	**12**	100	-4.51
	13	100	-4.75
	9	100	-3.31
	11	100	-4.25
6	**12**	100	-3.76
	13	100	-3.86
	9	100	-4.68
	11	100	-5.95
7	**12**	92	-5.03
	13	100	-4.76
	9	100	-1.77
	11	100	-2.68
8	**12**	100	-2.25

	13	100	-2.21
9	**9**	100	-3.51
	11	100	-4.09
	12	100	-3.98
	13	100	-4.17
10	**9**	100	-2.64
	11	69	-4.01
	12	75	-2.91
	13	85	-3.12
11	**9**	100	-2.11
	11	100	-3.80
	12	54	-2.28
	13	95	-2.32
12	**9**	100	-2.04
	11	100	-3.78
	12	36	-2.26
	13	63	-2.24
13	**9**	100	-3.96
	11	100	-4.62
	12	100	-4.01
	13	100	-4.30

Supplementary Table S3. Residues forming the most interesting pockets and HB donor residues.

Pocket ID	Residues	Hb donor residues
2	598 602 674 725 726 729 730 733 734 737 763 764 765 766 767 768 769 771	Tyr764, Ser674, His 726, Lys771
3	540 541 542 543 545 607 610 611 614 615 625 660 663	Tyr663, Arg614, Arg611, Tyr660
4	571 572 574 575 579 584 585 589 592 593 596 597 600 751 752 755 756 758 759 762	Gln597, Asn759, Lys579, Arg585, Gln592, Met593, Met572

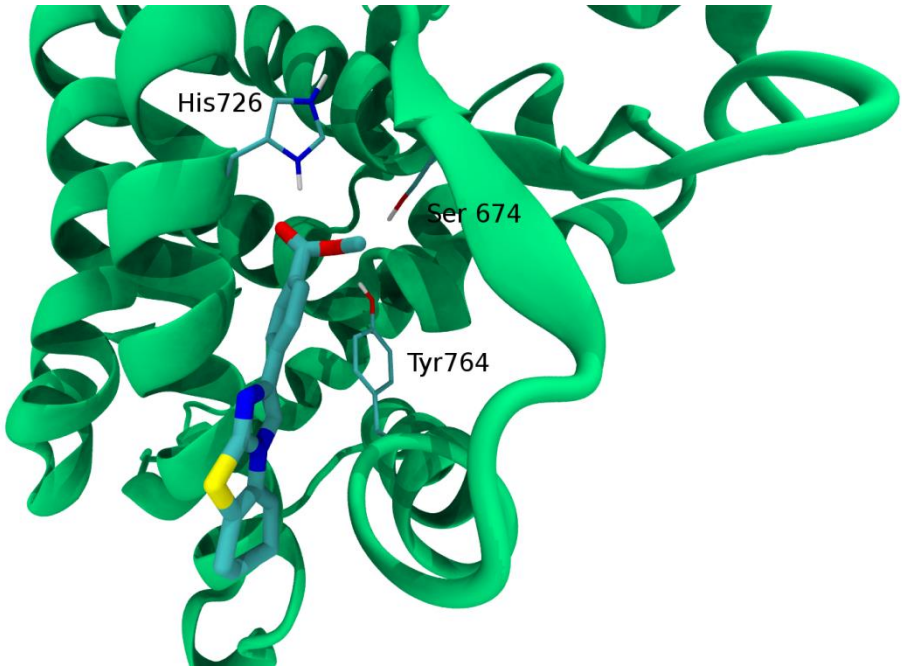

Supplementary Figure S3. Superimposition of docking poses of compounds **11** and **12** in pocket 2. The carboxyl and ester groups are oriented towards residues His 726, Ser 674 and Tyr 764, being able to form two HB with the highlighted residues.

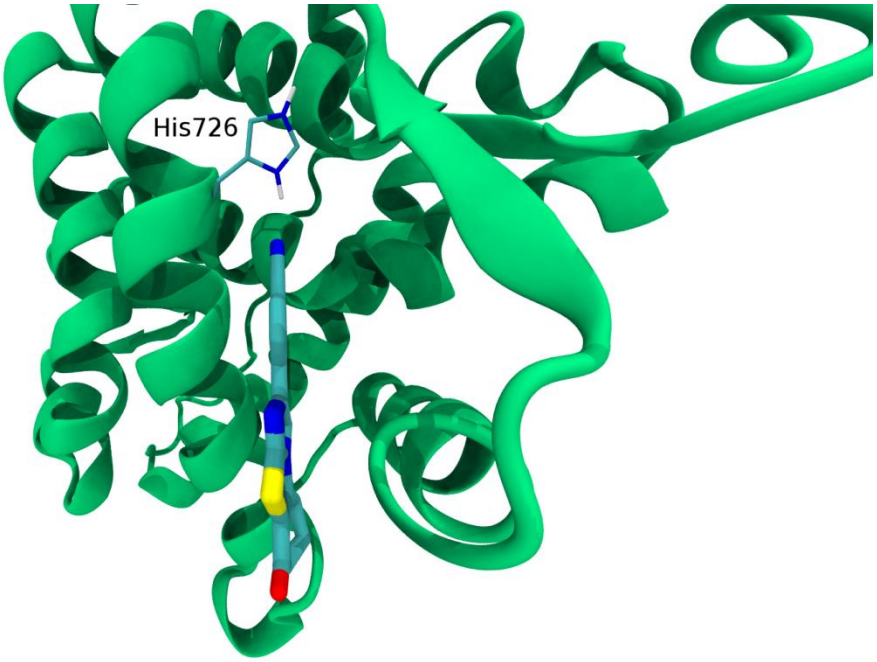

Supplementary Figure S4. Superimposition of docking poses of compounds **9** and **13** in pocket 2. Nitrile substituents are oriented towards residues His 726, forming a HB.

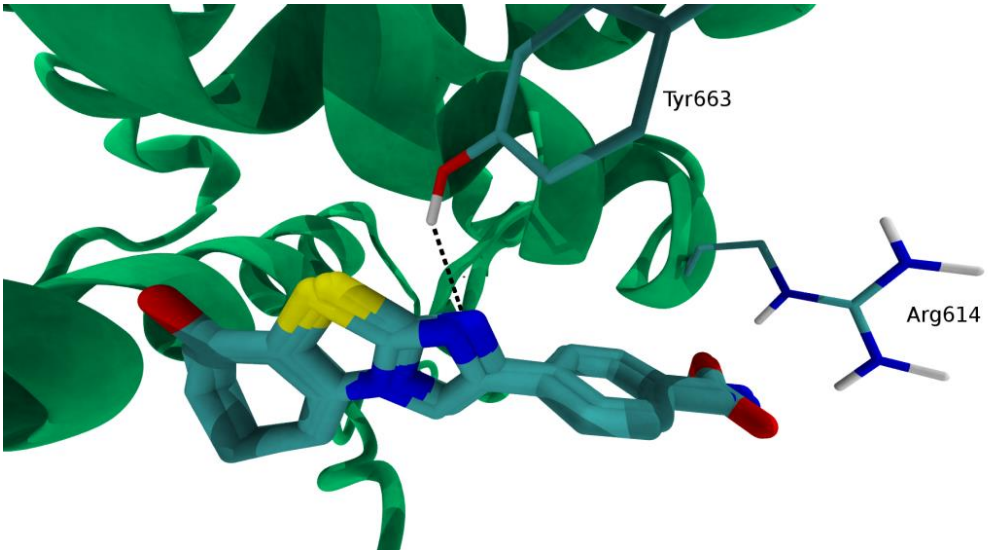

Supplementary Figure S5. Superimposition of docking poses of compounds **9**, **11**, **12** and **13** in pocket 3. HB between the acceptor nitrogen of all scaffolds is highlighted. Moreover, there is a salt bridge interaction between the carboxyl group of compound **11** and Arg 614.

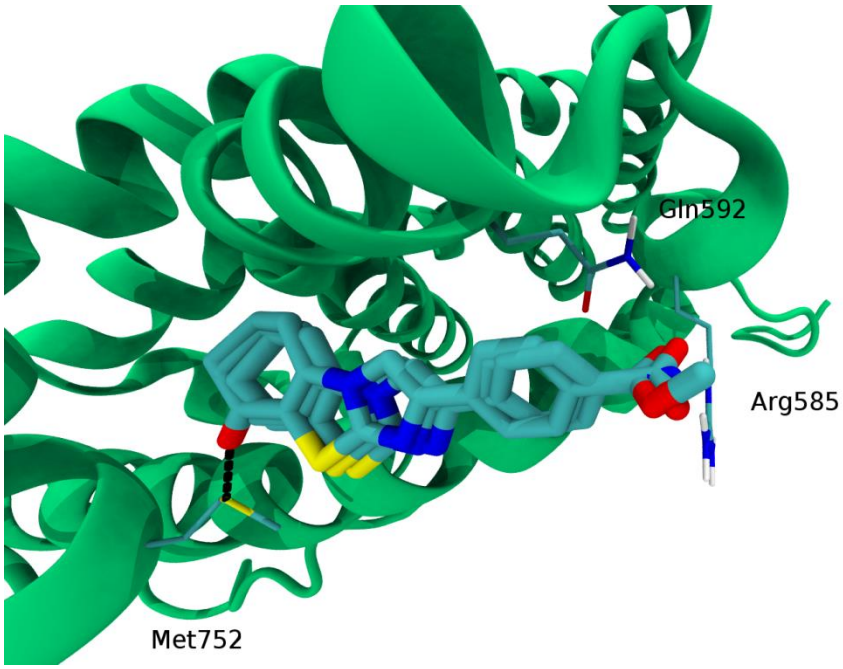

Supplementary Figure S6. Superimposition of docking poses of compounds **11**, **12** and **13** in pocket 4. Carboxyl group of **11** and Arg 585 forms a salt bridge. Carbonyl group of compound **13** interacts with Met 752 through a HB, while carbonyl groups of **11** and **12** form HBs with Gln 592.

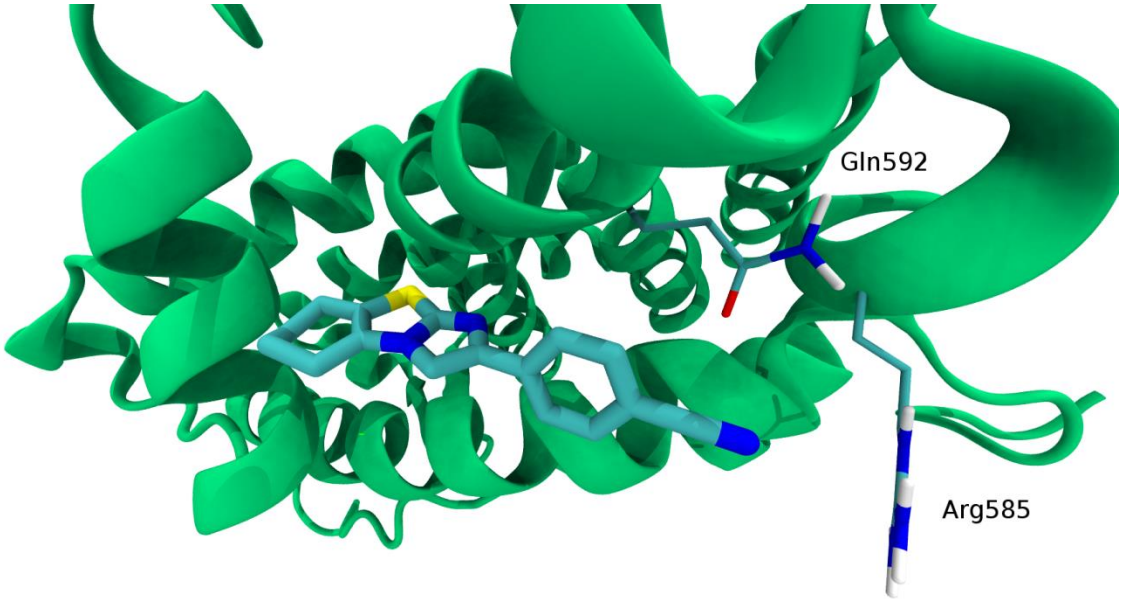

Supplementary Figure S7. Docking pose of compound 9 in pocket 4.

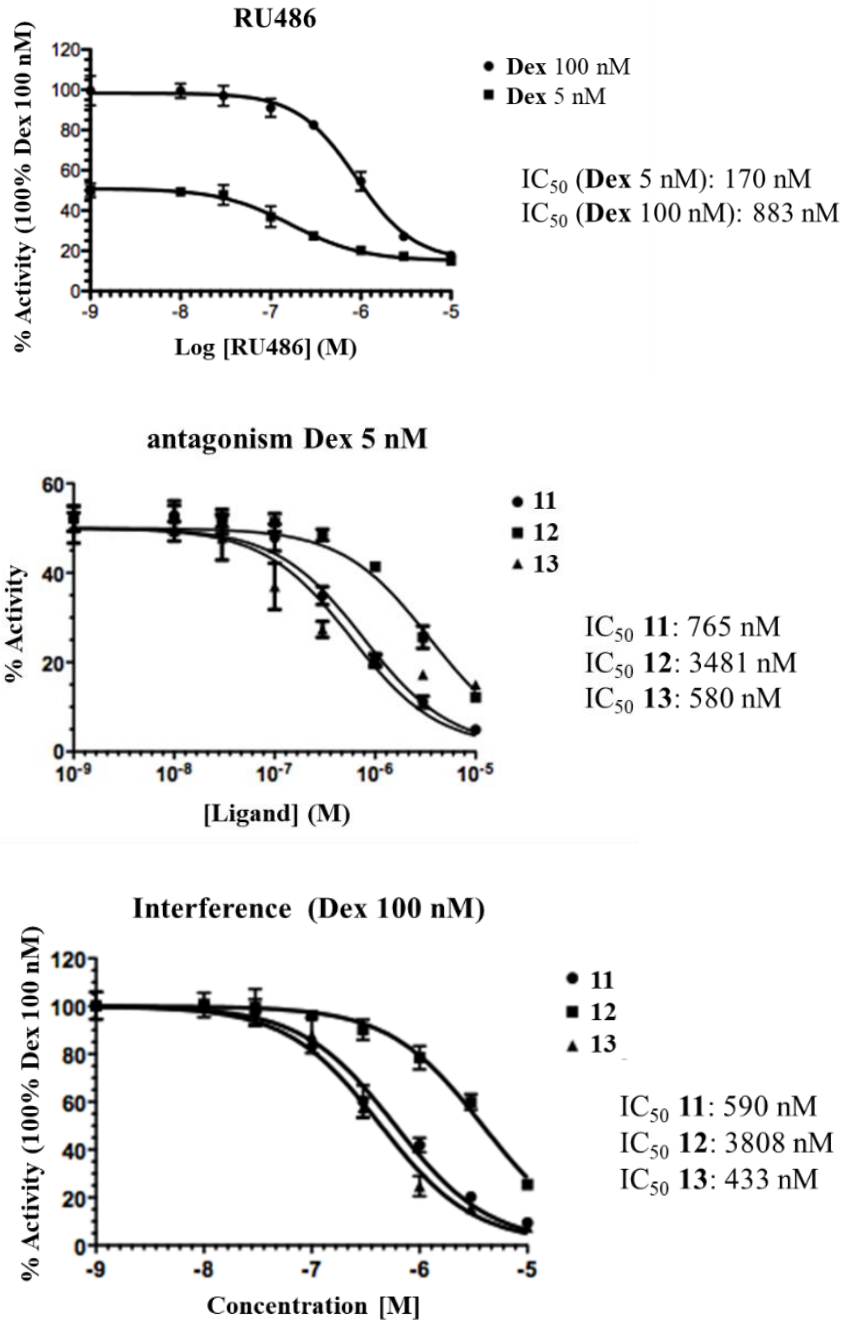

Supplementary Figure S8. GCR activity inhibition of compounds **11-13**.

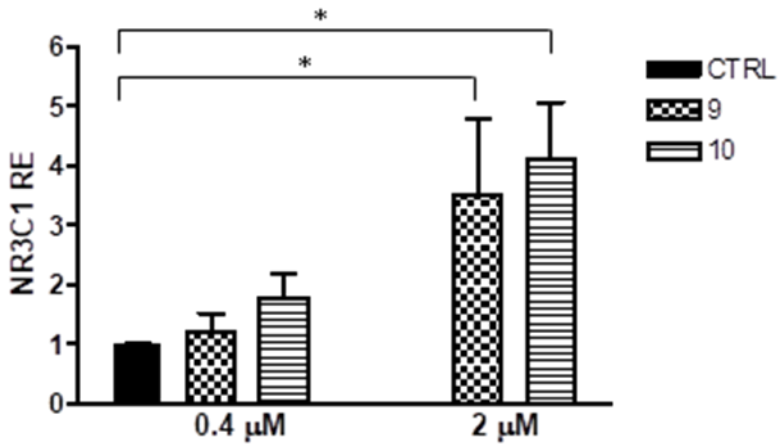

Supplementary Figure S9. GCR expression in HeLa cells after treatment with compounds **9** and **10** for 24 h at 0.4 and 2 µM. One-way ANOVA, 0.4 µM p = 0.525; 2 µM p = 0.041 and Bonferroni post Test vs CTRL * p-value<0.05. The data are reported as means ± SD of 3 independent experiments.

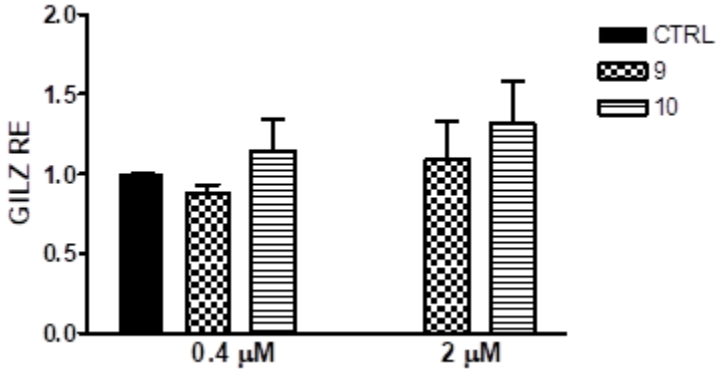

Supplementary Figure S10. GILZ expression in HeLa cells after treatment with compounds 9 and 10 for 24 h at 0.4 and 2 µM. One-way ANOVA, 0.4 µM p = 0.4905; 2 µM p = 0.5257. The data are reported as means ± SD of 3 independent experiments.

General structures of the tested compounds.

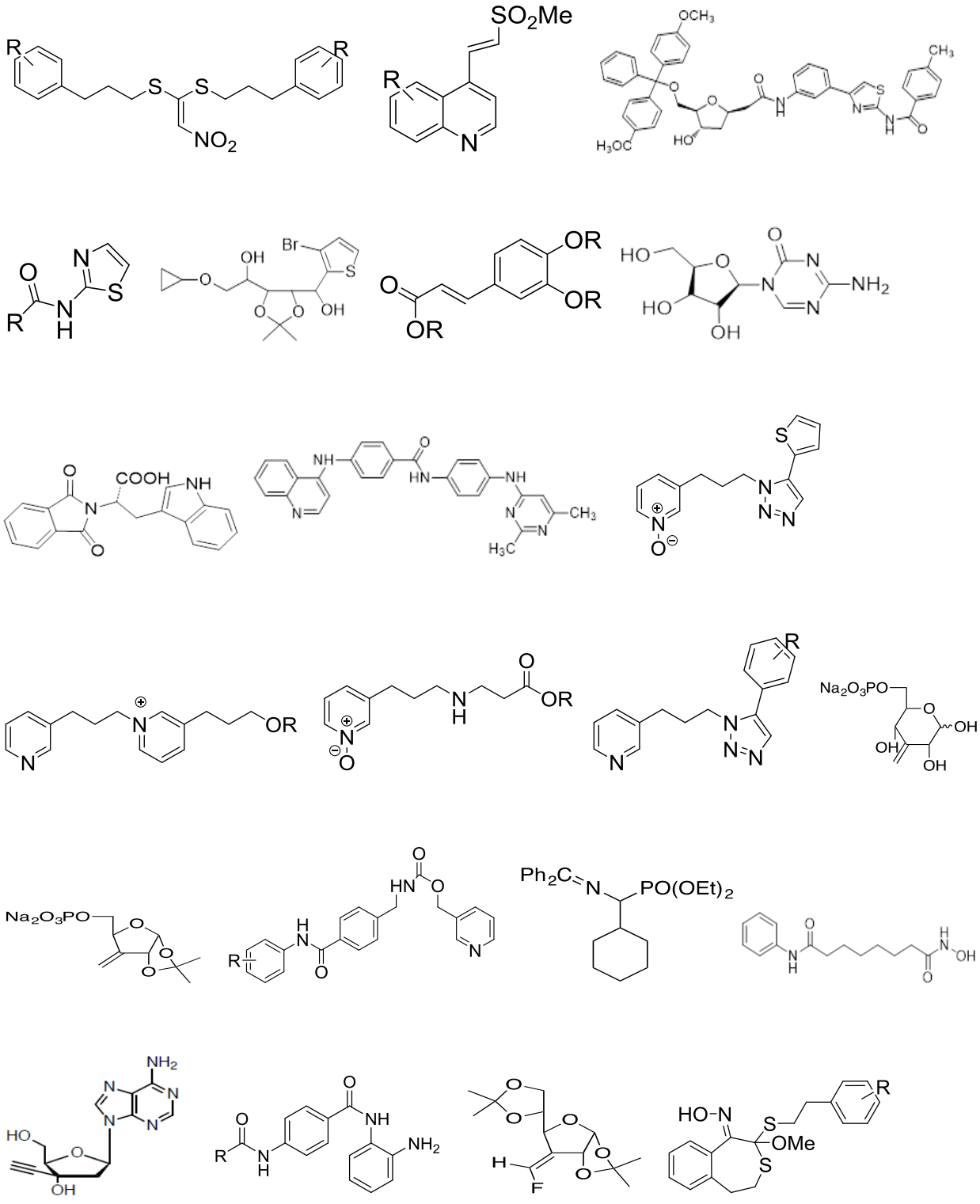

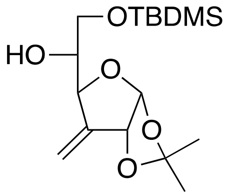
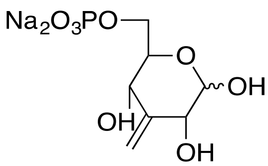
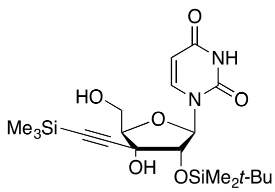
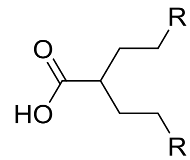
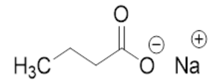

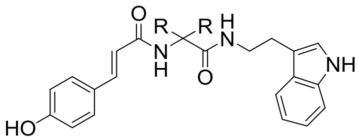
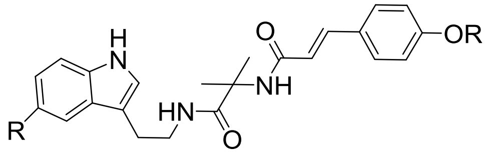
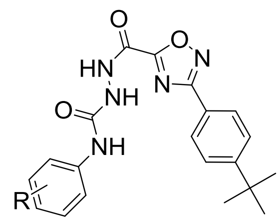

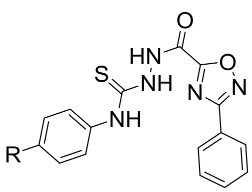
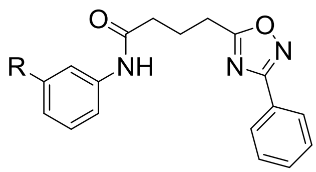
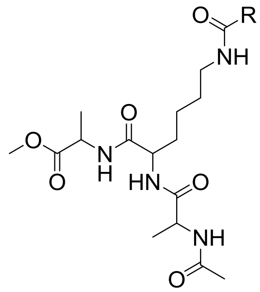
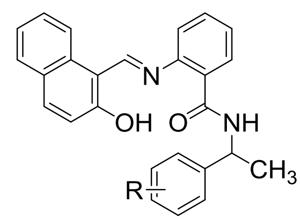

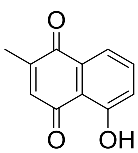
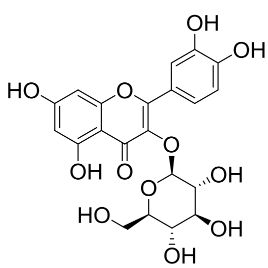
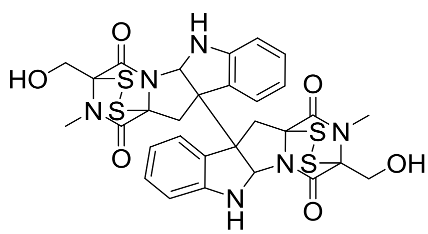
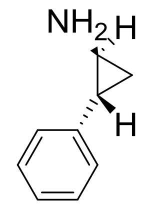
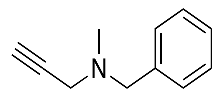

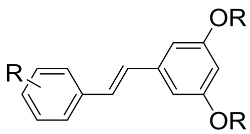
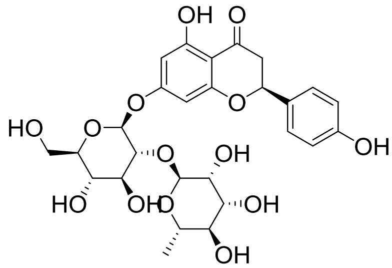
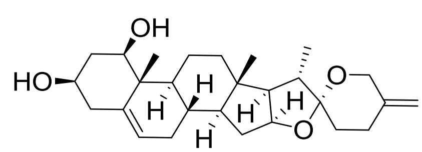

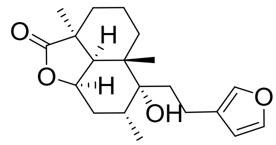
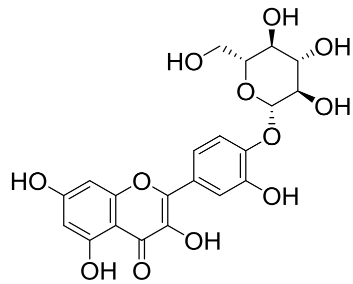
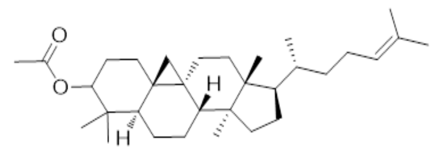

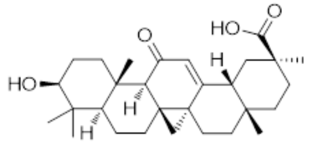
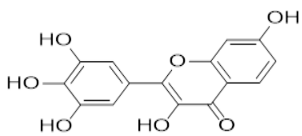
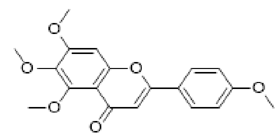
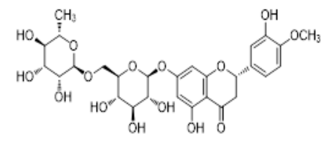

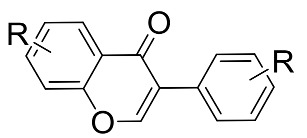
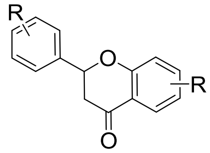
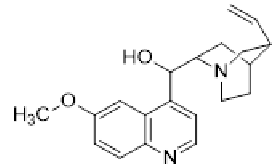
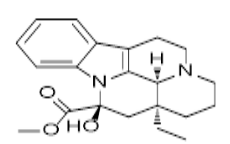

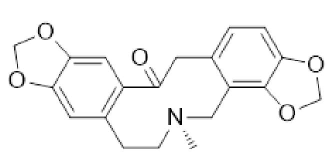
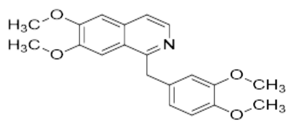
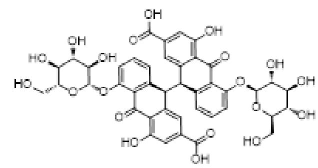
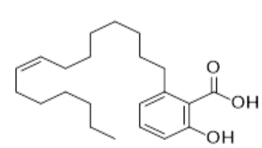

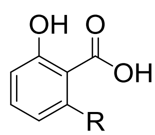
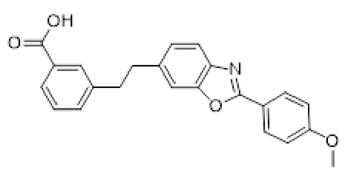
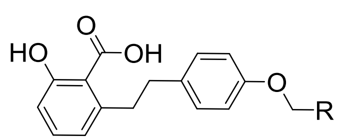
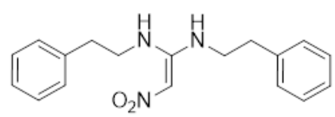

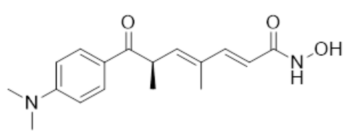
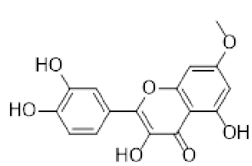
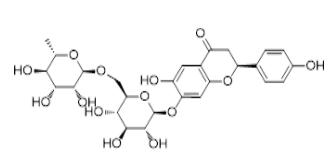
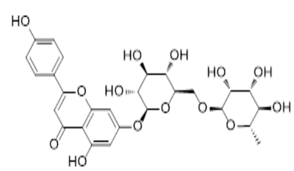

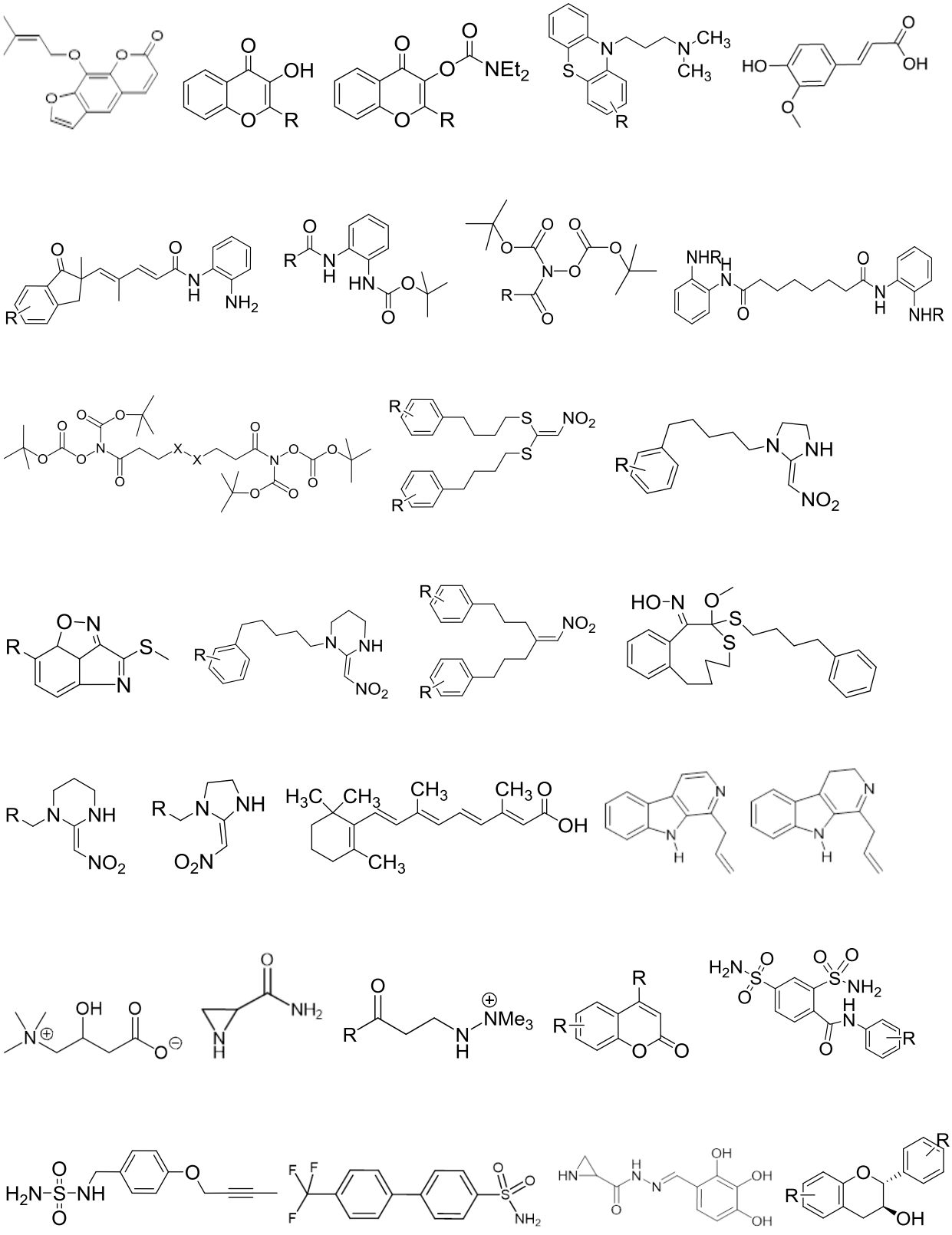

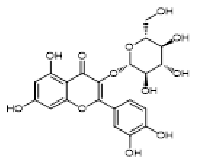
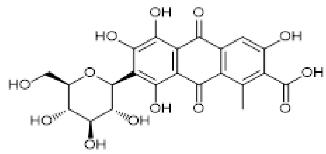
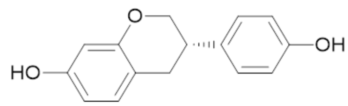
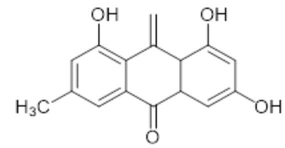

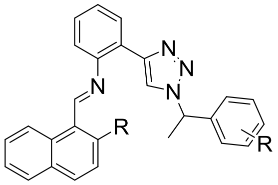
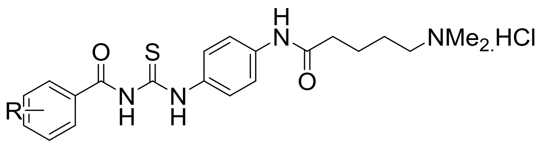
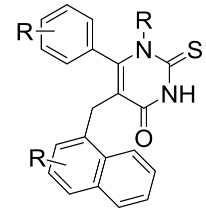
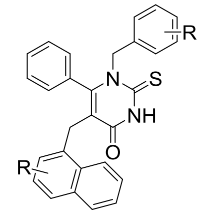

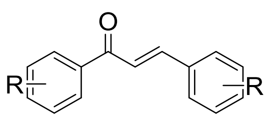
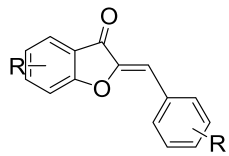
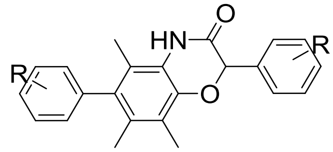
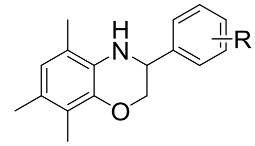

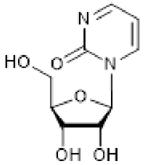
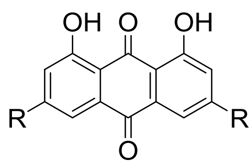
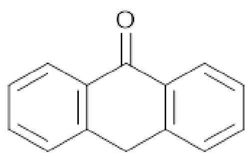
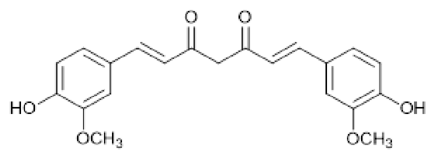

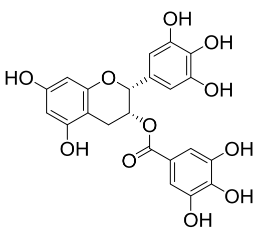
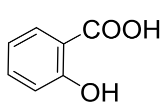
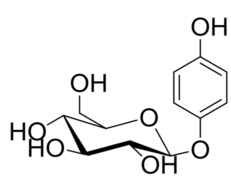
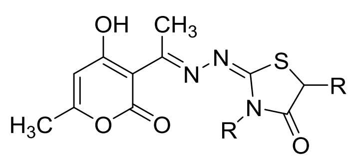
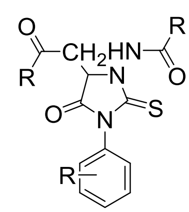

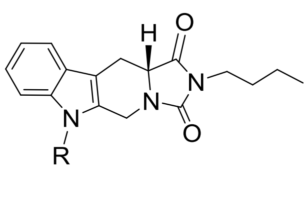
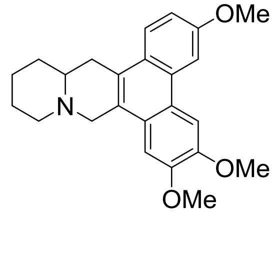
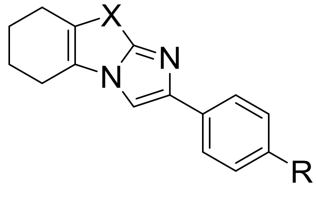
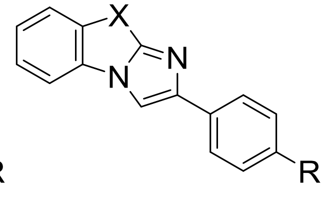

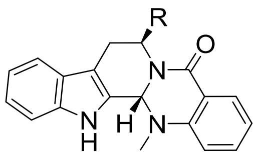
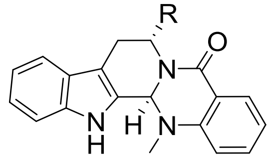
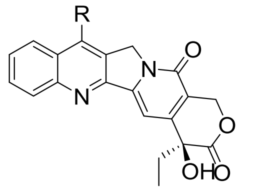
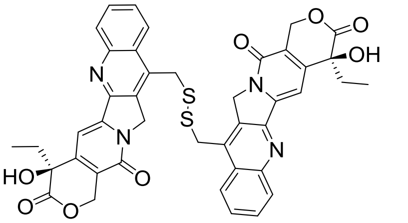
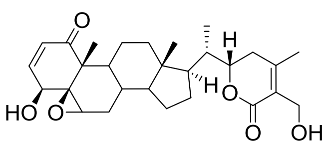
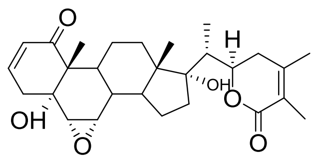
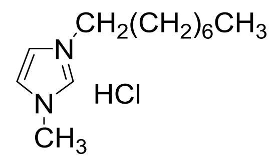
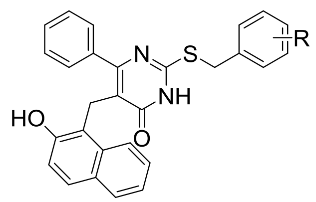
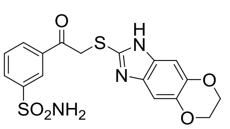
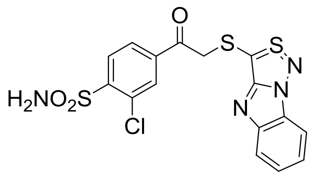
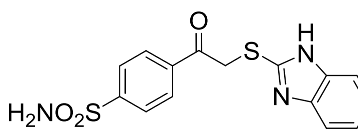
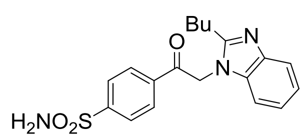
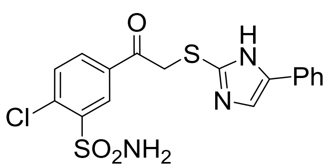
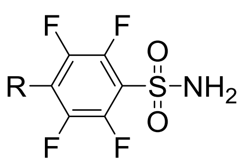
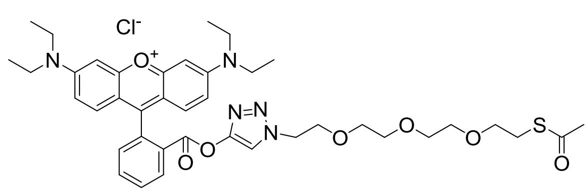
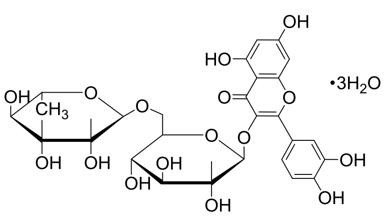
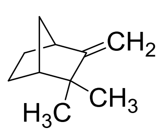
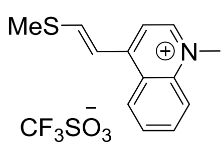
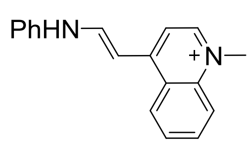
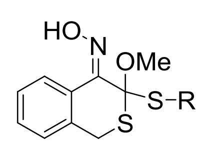
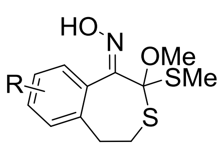
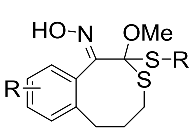
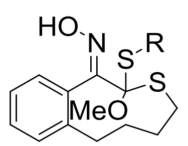
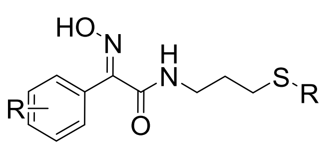
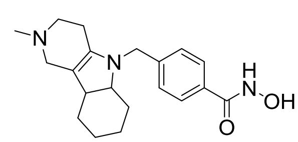

References:

1. Christodoulou, M. S.; Colombo, F.; Passarella, D.; Ieronimo, G.; Zuco, V.; De Cesare, M.; Zunino, F. Synthesis and biological evaluation of imidazolo[2,1-b]benzothiazole derivatives, as potential p53 inhibitors. *Bioorg. Med. Chem.* **2011**, *19*, 1649–1657.
2. McIntyre, N. A.; McInnes, C.; Griffiths, G.; Barnett, A. L.; Kontopidis, G.; Slawin, A. M. Z.; Jackson, W.; Thomas, M.; Zheleva, D. I.; Wang, S.; Blake, D. G.; Westwood, N. J.; Fischer, P. M.; Design, Synthesis, and Evaluation of 2-Methyl- and 2-Amino-N-aryl-4,5-dihydrothiazolo[4,5-*h*]quinazolin-8-amines as Ring-Constrained 2-Anilino-4-(thiazol-5-yl)pyrimidine Cyclin-Dependent Kinase Inhibitors. J. Med. Chem. 2010, 53, 2136–2145.
3. Bledsoe, R. K.; Montana, V. G.; Stanley, T. B.; Delves, C. J.; Apolito, C. J.; McKee, D. D.; Consler, T. G.; Parks, D. J.; Stewart, E. L.; Willson, T. M.; Lambert, M. H.; Moor, J. T.; Pearce, K. H.; Xu, H. E. Crystal structure of the glucocorticoid receptor ligand binding domain reveals a novel mode of receptor dimerization and coactivator recognition. *Cell*. **2002**, *110*, 93-105.
4. Morris, G. M.; Huey, R.; Lindstrom, W.; Sanner, M. F.; Belew, R. K.; Goodsell, D. S.; Olson, A. J. AutoDock4 and AutoDockTools4: Automated docking with selective receptor flexibility. *J. Comput. Chem*. **2009**, *30*, 2785-2791.
5. Morris, G. M.; Goodsell, D. S.; Halliday, R. S.; Huey, R.; Hart, W. E.; Belew, R. K.; Olson, A. J. Automated docking using a Lamarckian genetic algorithm and an empirical binding free energy function. *J. Comput. Chem*. **1998**, *19*, 1639-1662.
6. Humphrey, W.; Dalke, A.; Schulten, K. VMD: visual molecular dynamics. *J. Mol. Graphics*. **1996**, 14, 33-38.
7. Chirumamilla, C. S.; Palagani, A.; Kamaraj, B.; Declerck, K.; Verbeek, M. W. C.; Oksana, R.; De Bosscher, K.; Bougarne, N.; Ruttens, B.; Gevaert, K.; Houtman, R.; De Vos, W. H.; Joossens, J.; Van Der Veken, P.; Augustyns, K.; Van Ostade, X.; Bogaerts, A.; De Winter, H.; Vanden Berghe, W. Selective Glucocorticoid Receptor Properties of GSK866 Analogs with Cysteine Reactive Warheads. *Front. Immunol.* **2017**, *8*, 1324.
8. Yang, B. V.; Weinstein, D. S.; Doweyko, L. M.; Gong, H.; Vaccaro, W.; Huynh, T.; Xiao, H. Y.; Doweyko, A. M.; McKay, L.; Holloway, D. A.; Somerville, J. E.; Habte, S.; Cunningham, M.; McMahon, M.; Townsend, R.; Shuster, D.; Dodd, J. H.; Nadler, S. G.; Barrish, J. C. Dimethyl-diphenyl-propanamide derivatives as nonsteroidal dissociated glucocorticoid receptor agonists. *J. Med. Chem.* **2010**, *53*, 8241-8251.